Interlayer Josephson Coupling of Thermally Excited Vortices in $Bi_2Sr_2CaCu_2O_{8-y}$

Y. M. Wan, S. E. Hebboul, D. C. Harris, and J. C. Garland
Department of Physics, Ohio State University, Columbus, Ohio 43210
(Received 19 February 1993)

Measurements of the zero-field resistive transition of $Bi_2Sr_2CaCu_2O_8$ single crystals suggest that a bulk zero-resistance state develops through a sequential process characterized by two transition temperatures. The upper transition corresponds to Josephson coupling of parallel CuO bilayers, and the lower transition to the conventional Kosterlitz-Thouless dissociation of bound vortex excitations. Measurements using a "flux transformer" electrode geometry indicate a pronounced peak in the secondary voltage, which is suppressed by an external magnetic field.

PACS numbers: 74.40.+k, 74.50.+r, 74.60.Ge, 74.72.Hs

The unusual transport properties of the high temperature superconductor $Bi_2Sr_2Ca_1Cu_2O_{8-y}$ (BSCCO) highlight the importance of understanding the superconducting phase transition in strongly anisotropic materials. It is known [1] that the superconducting transition of this material shows quasi-two-dimensional behavior, as evidenced by an exponential square-root singularity in the temperature dependence of $\rho_{ab}(T)$, the electrical resistivity measured in the crystalline a-b plane, and by a power law in the current-voltage (IV) characteristics which increases from a linear (Ohmic) to a cubic dependence at T_c, and which becomes increasingly nonlinear at lower temperatures. Such behavior is commonly seen in two-dimensional superconducting films [2].

By contrast, along the c axis, the normal-state resistivity $\rho_c(T)$ of BSCCO is very high, of the order 10^5–10^6 of ρ_{ab}, with the thermally activated temperature dependence of a semiconductor and a broadened superconducting transition in which a critical current develops below T_c [3]. These properties are consistent with the view that superconductivity in BSCCO originates in stacked bilayers of CuO, oriented parallel to the a-b plane, with adjacent bilayers coupled by the Josephson interaction [4].

Although much recent work [5] has focused on the properties of quantized flux lines threading these bilayers, little is known about the details of the resistive transition. More generally, it is not yet established how the transition to bulk superconductivity proceeds in planar, anisotropic materials in which out-of-plane Josephson coupling modifies the conventional 2D transition [6]. Here, we address this issue through detailed measurements of the $H=0$ transition of BSCCO single crystals. We find that the development of a bulk zero-resistance state takes place through a sequential process characterized by two transition temperatures. At the upper transition temperature, designated T_c^c, the Josephson interaction couples two-dimensional CuO bilayers. At the lower transition temperature, designated T_c^{ab} (for BSCCO, $T_c^c - T_c^{ab} \approx 2$ K), the bilayers undergo a Kosterlitz-Thouless-type transition to a zero dissipation state. In the temperature interval $T_c^{ab} < T < T_c^c$, one has the curious phenomenon of Josephson supercurrents flowing between resistive two-dimensional planes.

Our transport measurements were performed on single crystals of BSCCO prepared by a standard solid state melt process [7]. A stoichiometric mixture of the oxides was placed inside a gold crucible and annealed at 900 °C in air for 5 h, followed by a slow cooling (1 °C/h) to 850 °C, at which time the oven was turned off. Samples were then annealed for 15 h at 600 °C in pure O_2 to improve the uniformity of the sample oxygenation. Typical sizes of cleaved crystals were 0.5 mm×1.0 mm×0.03 mm, with the c axis oriented along the thin dimension. Typical a-b plane and c-axis resistivities were $\rho_{ab}(100\ \text{K}) \approx 4.0\times10^{-4}\ \Omega$ cm, and $\rho_c \approx 1.5\ \Omega$ cm, in agreement with previously reported measurements on high quality crystals [8]. Figure 1 illustrates the temperature-dependent resistivities $\rho_c(T)$ and $\rho_{ab}(T)$ for a typical crystal.

Electrodes (up to six for each sample) were fabricated by bonding Au wires or foils to the crystal with Ag conductive paste (ACME Chemicals and Insulation Co., No. 3022) and by baking the samples in air for 1–2 h at 500–600 °C. The typical contact resistance of a completed electrode was 5 Ω or less. The inset to Fig. 1 illustrates the location of electrodes.

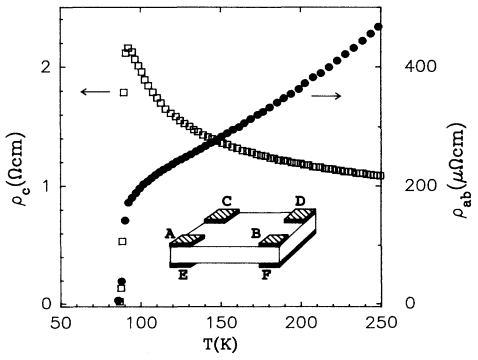

FIG. 1. T dependence of the $H=0$ a-b plane (ρ_{ab}) and c-axis (ρ_c) resistivities measured for sample 1. The inset shows the sample electrode geometry with the six contact pads designated A through F.

0031-9007/93/71(1)/157(4)$06.00

The samples were mounted inside a variable-temperature cryostat immersed in a ^{4}He bath. The cryostat was screened by superconducting Pb foil, with a residual internal magnetic field of less than 20 mG. Sample temperatures were monitored with a carbon-glass thermometer over the range 4–300 K. Temperatures were stabilized electronically between 4 and 110 K, and in this range absolute measurement accuracy was 0.1 K with a regulation stability of 20 mK or better.

Current-voltage and resistivity measurements were made using a four-terminal technique in which square wave currents (16.9 Hz) of 1 μA–50 mA were applied by a current source and the sample voltage detected with a lock-in amplifier whose resolution was 5×10^{-10} V. The data were recorded and stored digitally using a Data Precision Data-6000 recorder.

The extreme anisotropy of the normal-state resistivity of BSCCO presents special challenges in interpreting voltage measurements. In an anisotropic medium having $\rho_c \gg \rho_{ab}$, current injected into the a-b plane on a lateral face of the crystal is confined to a thin region near the surface of that face; for our samples, the lines of current are "squeezed" by a factor of $(\rho_{ab}/\rho_c)^{1/2} \approx 10^{-3}$ compared to the distribution in an isotropic medium. Because of this nonuniformity, it is necessary to deduce the planar resistivity ρ_{ab} from the solutions of Laplace's equation for our particular electrode configuration; Busch *et al.* [9] have recently discussed this point in detail. The normal-state resistivity data for ρ_{ab} in Figs. 1 and 3 are based on an analysis of the potential distribution using the Busch *et al.* methodology.

Another complication is illustrated in Fig. 2, which shows a family of logarithmic IV characteristics taken in a narrow temperature range near the superconducting transition. Figure 2(a) shows the voltage V_c, measured between electrodes A and E, when current is injected into electrodes B-F, while Fig. 2(b) shows the voltage V_{ab} measured between electrodes A and B for current injected into electrodes C-D. At higher temperatures, the normal-state IV characteristics in both figures have a linear slope, as expected. However, at lower temperatures, the onset of superconductivity is not marked by a clear zero-voltage state, but rather by the development of nonlinearities in the IV characteristics at low current densities. In interpreting our measurements, we have therefore defined T_c for the resistive transition to be the temperature below which the IV characteristics show nonlinear behavior with a differential slope greater than unity. The solid lines in Figs. 2(a) and 2(b) show the section of the IV characteristics from which our estimates of T_c were determined.

In Fig. 2(a), the data are dominated by the c-axis resistivity ρ_c, and the nonlinearity takes the form of a gradually increasing slope as the current is reduced [10]. In Fig. 2(b), the data are dominated by the planar resistivity ρ_{ab}. Here, the important feature is the existence of

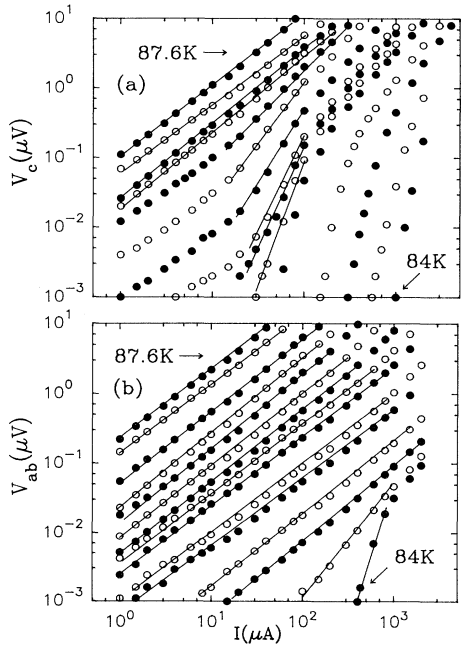

FIG. 2. T dependence of IV characteristics for sample 1 using two lead configurations. (a) V_{AE} vs I_{BF} (J$\|$c axis) and (b) V_{AB} vs I_{CD} (J$\perp$c axis), for T = 87.6, 87.1, 86.8, 86.6, 86.4, 86.2, 85.9, 85.6, 85.4, 85.2, 85.0, 84.7, 84.4, 84.2, and 84.0 K, respectively.

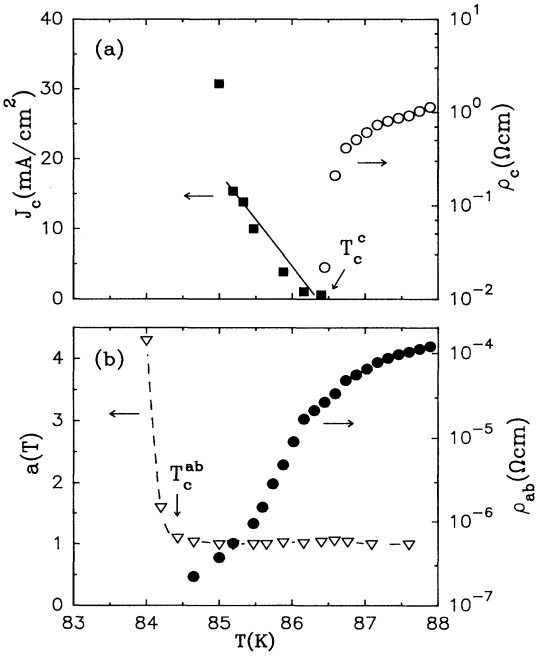

FIG. 3. Expanded T dependence for sample 1 showing (a) ρ_c and J_c deduced from Fig. 2(a) and (b) ρ_{ab} and the IV exponent a obtained from Fig. 2(b).

linear IV characteristics in the curves down to nearly 84 K, a temperature about 2 K below that at which nonlinearity became evident in the ρ_c characteristics of Fig. 2(a).

Figures 3(a) and 3(b) show an expanded view of the resistive transition for $\rho_c(T)$ and $\rho_{ab}(T)$, respectively. In Fig. 3(a), $\rho_c(T)$ (right-hand scale) shows an abrupt transition to zero at $T_c^c \approx 86.4$ K. At lower temperatures, a c-axis critical current $I_c^c(T)$ (left-hand scale) develops; the values of $I_c^c(T)$ were obtained by extrapolating the IV characteristics of Fig. 2(a) to 1 nV, a procedure which is likely to underestimate the actual critical current. In contrast, $\rho_{ab}(T)$, shown in Fig. 3(b) (right-hand scale), displays a broadened resistive transition, with $T_c^{ab} \approx 84.3$ K. Also shown in Fig. 3(b) is the exponent of the IV characteristics $a(T)$ (left-hand scale), showing the sharp onset of nonlinear behavior at T_c^{ab} [11].

Figures 4(a) and 4(b) illustrate the transport behavior of BSCCO in the ≈ 2 K temperature region between T_c^c and T_c^{ab}, where the crystal shows zero resistivity along the c axis but is still resistive in the a-b plane. These data, obtained by injecting a dc bias current into the a-b plane on the top face of the crystal (electrodes A-B) while detecting the voltage on the bottom face (electrodes E-F), show that there is a pronounced peak in the detected voltage $V_s(T)$ within this temperature range. Figure

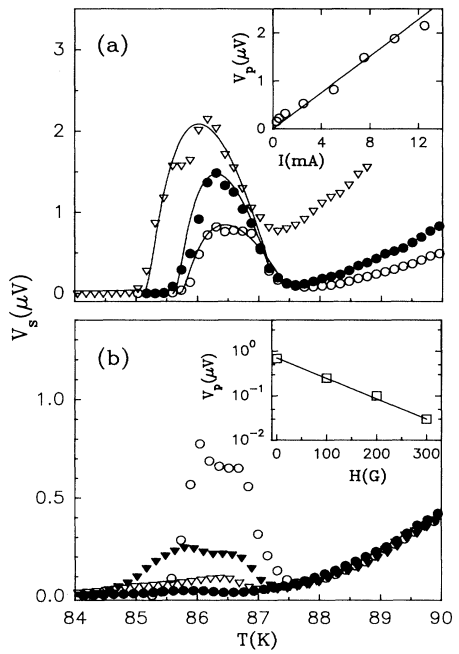

FIG. 4. T dependence of the secondary voltage V_s for sample 2. (a) $V_s(T)$ for $I_{primary}=5.0$ mA (○), 7.5 mA (●), and 12.5 mA (▽), and $H=0$. The curves are model fits. The inset shows V_{peak} vs $I_{primary}$. (b) $V_s(T)$ for H ($\|a$-b plane)$=0$ G (○), 100 G (▼), 200 G (▽), and 300 G (●), and $I_{primary}=5.0$ mA. The inset shows V_{peak} vs H.

4(a) illustrates the temperature dependence of the voltage for various values of dc bias current, with the inset illustrating a linear dependence of the maximum peak voltage V_{peak} with current. It is also apparent from the figure that the position of V_{peak} shifts to lower temperatures and that the peak becomes broader as the bias current increases. Figure 4(b) shows the effect on the detected voltage of an external magnetic field applied parallel to the a-b plane. The inset illustrates the suppression of the peak amplitude V_{peak} with increasing field.

The electrode configuration used for the data of Fig. 4 is sometimes called a "transformer" geometry [12], to reflect the idea that the two-dimensional CuO_2 planes in BSCCO can be magnetically coupled (by vortex lines), even though they may be electrically isolated from each other. Our results, however, point to a picture of the conduction mechanism in the temperature range $T_c^{ab} < T < T_c^c$ that is more complicated than that suggested by this transformer analogy. Specifically, the existence of the peak structure in the voltage across the transformer "secondary" electrodes [Figs. 4(a) and 4(b)] indicates that the resistive behavior of the crystal is not a result merely of the a-b planes being short circuited by the zero c-axis resistivity. Instead, we believe that the peak results from the tendency of the interplane Josephson interaction to align thermally excited (Kosterlitz-Thouless) vortex excitations on adjacent a-b planes [13].

According to our view, there is an appreciable quantum coupling of vortex phases on adjacent planes resulting from the interplane Josephson interaction [6]. (Note that the magnetic coupling between layers is very small since, to lowest order, the magnetization of each layer is zero.) This interaction energy is minimized if the centers of vortex phase on adjacent planes are aligned; any vortex misalignment, as might arise because of a transport current, raises the energy and results in a restoring force, the magnitude of which is proportional to the c-axis Josephson critical current.

In the measurements of Figs. 4(a) and 4(b), a current applied along the top face of the crystal drives the vortex excitations in that layer at constant velocity [14]. Because of the interplane Josephson interaction, however, excitations on other a-b planes will also be dragged along by this current. The signal voltage on the bottom layer will be proportional to the density of free vortex excitations, the interplane Josephson coupling energy, and the applied current. According to this picture, the peak effect in the detected voltage thus results from the competition between the temperature dependence of the free vortex density, which increases exponentially with temperature above T_c^{ab}, and that of the Josephson coupling energy, which decreases smoothly to zero as T_c^c is approached from below. Our model is also qualitatively consistent with the linear current response of the voltage peak [Fig. 4(a), inset] and the suppression of the peak with external magnetic field [Fig. 4(b), inset], the latter

resulting from the field-dependent depression of the Josephson interaction energy [15].

Our model may be placed on a semiquantitative footing by setting the coupling energy E_c of two thermally excited vortices located in adjacent Josephson-coupled CuO bilayers to be proportional to the Josephson coupling energy $E_J = \hbar I_c^c/2e$, yielding $E_c \propto I_c^c$, where I_c^c is the c-axis critical current. The latter is shown in Fig. 3(a) and is found to display an approximate linear temperature dependence near T_c^c, i.e., $I_c^c(T) \propto 1 - T/T_c^c$. In addition, we use the Halperin-Nelson [16] expression for the density of thermally dissociated vortices,

$$n_F(T) \approx C\xi(T)^{-2}\exp\{-2[b(T_{c0}-T_c^{ab})/(T-T_c^{ab})]^{1/2}\},$$

which is valid in the temperature range $T_c^{ab} < T < T_{c0}$, where T_{c0} is the mean-field transition temperature and C and b are nonuniversal constants. The flux-flow resistance resulting from a small bias current I is given by $R(T) = 2\pi R_n \xi(T)^2 n_F(T)$, where R_n is the normal-state resistance, and produces a "primary" voltage $V_p(T) = R(T)I$.

The "secondary" voltage is given by $V_s(T) = \alpha(T)V_p(T)$, with the phenomenological coupling constant $\alpha(T) \propto I_c^c(T)$ and $0 \le \alpha(T) \le 1$. Near T_c^c, we assume the form $\alpha(T) \approx \alpha_0 \exp(-d/d_0)(1 - T/T_c^c)$, where d is the sample thickness. To obtain the thickness dependence, we estimate the ratio $V_s/V_p \sim 0.05$ and 0.55, at $T \sim 0.99T_c^c$, for samples 1 ($d_1 \sim 30$ μm) and 2 ($d_2 \sim 10$ μm), respectively, and deduce a characteristic length $d_0 \sim 8$ μm, with a coefficient $\alpha_0 \sim 200$. The curves shown in Fig. 4(a) for sample 2 were then obtained by setting $R_n = 1.0$ mΩ, $b = 1.0$, and $T_{c0} = T_c^c$ in the expression for $V_s(T)$. The fits yielded good agreement with the data for $C \approx 0.77 \pm 0.10$, $T_{c0} \approx 87.2$ K, and $T_c^{ab} \approx 85.2 \pm 0.4$ K.

Finally, we find that an external magnetic field suppresses the secondary voltage [Fig. 4(b)]. A qualitative interpretation of this result is obtained as follows. For $H \| a$-b planes, the c-axis critical current is suppressed, yielding a smaller secondary voltage. For $H \perp a$-b planes, however, the higher free vortex density produces a larger in-plane vortex-vortex interaction which then weakens the out-of-plane vortex coupling strength [12,17]. In this case, the a-b plane critical temperature, T_c^{ab}, is also expected to be lowered due to vortex screening [18].

We are indebted to L. N. Bulaevskii, J. R. Clem, V. G. Kogan, W. E. Lawrence, M. Ledvij, and J. W. Wilkins for many helpful discussions. This work was supported by DOE (MISCON) through Contract No. DE-FG02-90ER45427 and by NSF Grant No. DMR 92-00122.

[1] S. Martin, A. T. Fiory, R. M. Fleming, G. P. Espinosa, and A. S. Cooper, Phys. Rev. Lett. **62**, 677 (1989); S. N. Artemenko, I. G. Gorlova, and Yu. I. Latyshev, Pis'ma Zh. Eksp. Teor. Fiz. **49**, 566 (1989) [JETP Lett. **49**, 654 (1989)].

[2] J. E. Mooij, *Percolation, Localization and Superconductivity*, edited by A. M. Goldman and S. A. Wolf (Plenum, New York, 1983), p. 325, and references therein.

[3] S. Martin, A. T. Fiory, R. M. Fleming, G. P. Espinosa, and A. S. Cooper, Appl. Phys. Lett. **54**, 72 (1989).

[4] R. Kleiner, F. Steinmeyer, G. Kunkel, and P. Müller, Phys. Rev. Lett. **68**, 2394 (1992).

[5] G. Briceno, M. F. Crommie, and A. Zettl, Phys. Rev. Lett. **66**, 2164 (1991); H. Safar, P. L. Gammel, D. J. Bishop, D. B. Mitzi, and A. Kapitulnik, Phys. Rev. Lett. **68**, 2672 (1992); L. N. Bulaevskii, M. Ledvij, and V. G. Kogan, Phys. Rev. Lett. **68**, 3773 (1992).

[6] P. Minnhagen and P. Olsson, Phys. Rev. Lett. **67**, 1039 (1991), and references therein.

[7] J. M. Imer *et al.*, Phys. Rev. Lett. **62**, 336 (1989).

[8] J. R. Cooper, L. Forro, and B. Kesaei, Nature (London) **343**, 444 (1990).

[9] R. Busch, G. Ries, H. Werthner, G. Kreiselmeyer, and G. S. Ischenko, Phys. Rev. Lett. **69**, 522 (1992).

[10] For the curves very near T_c, the data show linear behavior at high currents, a region of nonlinear behavior at intermediate currents, and a return to a residual linearity at the lowest currents; this behavior is consistent with the effect of thermal fluctuations on Josephson critical currents [V. Ambegaokar and B. I. Halperin, Phys. Rev. Lett. **22**, 1364 (1969)].

[11] In a two-dimensional transition, the exponent $a(T)$ for the planar resistivity ρ_{ab} is expected to show a discontinuous jump from 1 to 3 at T_c. For these data, $a(T)$ shows a more marked discontinuity, which results from the nonuniform current distribution in the sample. Using a different lead geometry, in which current is uniformly injected into the Cu-O planes, we have independently verified that the $a(T)$ behaves as expected.

[12] J. W. Ekin and J. R. Clem, Phys. Rev. B **12**, 1753 (1975).

[13] Busch *et al.* (Ref. [9]) recorded a structure in their $\rho_{bot}(T)$ curves which resembled our secondary voltage peak. The authors briefly stated that the knee in $\rho_c(T)$ close to T_c gave rise to a dip in $\rho_{bot}(T)$. Our findings, however, show that the secondary voltage peak appears between T_c^{ab} and T_c^c, with the dip in $V_s(T)$ lying several degrees below the knee in $\rho_c(T)$.

[14] J. Bardeen and M. J. Stephen, Phys. Rev. **140**, A1197 (1965).

[15] D. I. Glazman and A. E. Koshelev, Zh. Eksp. Teor. Fiz. **97**, 1371 (1990) [Sov. Phys. JETP **70**, 774 (1990)].

[16] B. I. Halperin and D. R. Nelson, J. Low Temp. Phys. **36**, 599 (1979).

[17] Recently, H. Safar, E. Rodriguez, F. de le Cruz, P. L. Gammel, L. F. Schneemeyer, and D. J. Bishop, Phys. Rev. B **46**, 14238 (1992), observed a decoupling of "pancake" vortices in adjacent CuO bilayers for H parallel to the c axis, in agreement with our results.

[18] J. C. Garland and Hu Jong Lee, Phys. Rev. B **36**, 3638 (1987).